The Astrophysical Journal Supplement Series, 154:54–59, 2004 September

FIRST INSIGHTS INTO THE *SPITZER* WIDE-AREA INFRARED EXTRAGALACTIC LEGACY SURVEY (SWIRE) GALAXY POPULATIONS

Carol Lonsdale,[1] Maria del Carmen Polletta,[2] Jason Surace,[1] Dave Shupe,[1] Fan Fang,[1] C. Kevin Xu,[1] Harding E. Smith,[2] Brian Siana,[2] Michael Rowan-Robinson,[3] Tom Babbedge,[3] Seb Oliver,[4] Francesca Pozzi, Payam Davoodi,[4] Frazer Owen,[5] Deborah Padgett,[2] Dave Frayer,[2] Tom Jarrett,[2] Frank Masci,[2] JoAnne O'Linger,[2] Tim Conrow,[2] Duncan Farrah,[6] Glenn Morrison,[6] Nick Gautier,[6] Alberto Franceschini,[7] Stefano Berta,[7] Ismael Perez-Fournon,[8] Evanthia Hatziminaoglou,[8] Alejandro Afonso-Luis,[8] Herve Dole,[9] Gordon Stacey,[10] Steve Serjeant,[11] Marguerite Pierre,[12] Matt Griffin,[13] and Rick Puetter[2]

Received 2004 April 5; accepted 2004 June 7

ABSTRACT

We characterize the *Spitzer* Wide-area Infrared Extragalactic Legacy Survey (SWIRE) galaxy populations in the SWIRE validation field within the Lockman Hole, based on the 3.6–24 μm *Spitzer* data and deep U, g', r', i' optical imaging within an area $\sim$1/3 deg^2 for $\sim$16,000 *Spitzer* SWIRE sources. The entire SWIRE survey will discover over 2.3 million galaxies at 3.6 μm and almost 350,000 at 24 μm; $\sim$70,000 of these will be five-band 3.6-24 μm detections. The colors cover a broad range, generally well represented by redshifted spectral energy distributions of known galaxy populations; however, significant samples of unusually blue objects in the [3.6]$-$[4.5] color are found, as well as many objects very red in the 3.6$-$24 μm mid-IR. Nine of these are investigated and are interpreted as star-forming systems, starbursts, and active galactic nuclei (AGNs) from $z = 0.37$ to 2.8, with luminosities from $L_{\rm IR} = 10^{10.3}$ to $10^{13.7}$ $L_\odot$.

Subject headings: galaxies: evolution — infrared: galaxies

1. INTRODUCTION AND OBSERVATIONS

The *Spitzer* Wide-area Infrared Extragalactic Legacy Survey (SWIRE; Lonsdale et al. 2003), will map the evolution of spheroids, disks, starbursts, and active galactic nuclei (AGNs) to $z > 2$, within volumes large enough to sample the largest important size scales (Oliver et al. 2004). We present initial results from deep optical (U, g', r', i') and *Spitzer* SWIRE (3.6–24 μm) imaging of 0.3 deg^2 in the SWIRE Survey validation field (VF) in the Lockman Hole, a field selected to have extremely low cirrus emission and a lack of bright radio sources. Deep K-band and VLA 20 cm imaging also exist, and this field will be imaged with *Chandra* ACIS-I to 70 ks depth in 2004 August. The full SWIRE survey will image $\sim$49 deg^2 in all Infrared Array Camera (IRAC) and Multiband Imaging Photometer (MIPS) bands in six fields. The area has been reduced from the strategy described by Lonsdale et al. (2003) in order to maintain two high-quality coverages of each field with the MIPS 70 μm array.[14] The SWIRE validation field was imaged by *Spitzer* in 2003 December following the strategy described in Lonsdale et al. (2003), so it has a shallower MIPS depth than the main SWIRE survey. The full SWIRE Lockman field was imaged with the new strategy in 2004 April and May.

The SWIRE VF is centered at $10^{\rm h}46^{\rm m}$, $+59^\circ01'$. The observations were executed on 2003 December 5 and 9. The *Spitzer* Program ID (PID) for these data is 142, and the data sets are identified as IRAC AOR key 0007770880, 0007771136, and MIPS AOR key 0007770368, 0007770624. Data processing began with the *Spitzer* Basic Calibrated Data (BCD) products, which are individual *Spitzer* images corrected for bias offsets and pixel-to-pixel gain variations (flat-fielding) and flux-calibrated in surface brightness units of MJy sr^{-1}. Additional individual IRAC image processing corrected latent images and electronic offset effects. For MIPS, scan-mirror–dependent flats were derived from the data and applied to the BCD images. The individual images, which have measurable spatial distortions, were reprojected onto a single common projection system on the sky, and then co-added through averaging with outlier rejection to remove cosmic-ray and other transient artifacts. A three-color 3.6, 4.5, 24 μm false-color image of part of the field is shown in Figure 1 (Plate 1).

Fluxes were extracted in 5.″8 apertures for IRAC ($\sim$2–3 times the FWHM beam) and 12″ for MIPS 24 μm, using SExtractor. Very few (<5%) of the detected objects are extended relative to the large *Spitzer* beams (>2″ at the shortest wavelength), and even fewer on scales comparable to the

[1] Infrared Processing and Analysis Center, California Institute of Technology, MC 100-22, Pasadena, CA 91125.
[2] Center for Astrophysics and Space Sciences, University of California, San Diego, La Jolla, CA 92093–0424.
[3] Astrophysics Group, Blackett Laboratory, Imperial College, Prince Consort Road, London SW7 2BW, UK.
[4] Astronomy Centre, CPES, University of Sussex, Falmer, Brighton BN1 9QJ, UK.
[5] National Radio Astronomy Observatory, P.O. Box O, Socorro, NM 87801.
[6] Jet Propulsion Laboratory, MC 264-767, 4800 Oak Grove Drive, Pasadena, CA 91109.
[7] Dipartimento di Astronomia, Universita di Padova, Vicolo Osservatorio 5, I-35122 Padua, Italy.
[8] Instituto de Astrofisica de Canarias, 38200 La Laguna, Tenerife, Spain.
[9] Institut d'Astrophysique Spatiale, Universite Paris Sud bat 121, F-91405 Orsay, France.
[10] Department of Astronomy, Cornell University, 220 Space Science Building, Ithaca, NY 14853.
[11] Centre for Astronomy and Planetary Science, School of Physical Sciences, University of Kent at Canterbury, Canterbury, Kent CT2 7NZ, UK.
[12] CEA/DSM/DAPNIA, Service d'Astrophysique, 91191 Gif-sur-Yvette, France.
[13] Department of Physics and Astronomy, University of Wales Cardiff, 5 The Parade, Cardiff CF24 3YB, UK.

[14] See http://www.ipac.caltech.edu/SWIRE for details.

TABLE 1
Spitzer Sensitivities and Detection Statistics

Parameter	λ_c (μm)							
	3.6	4.5	5.8	8	24	3.6, 4.5	All IRAC	All IRAC, 24
5 σ limit, validation field (μJy)	3.7	5.3	48	37.7	150	...	...	...
All detections, 0.3 deg^2, VF	16,075	12,675	1536	1657	1290	11,765	950	433
Galaxies (stars removed statistically)	14,630	11,403	1091	1247	1283	10,706	760	430
5 σ limit, full survey (μJy)	3.7	5.3	48	37.7	106	...	...	...
Predicted galaxies, 49 deg^2 ($\times 10^6$)	2.39	1.86	0.18	0.20	0.35	1.75	0.12	0.07
Model, 49 deg^2, Xu et al. (2003) S3+E2	6.36	4.76	0.24	0.33	0.72	4.75	0.21	0.17
Projected/Model	0.38	0.39	0.75	0.61	0.49	0.37	0.57	0.41

extraction apertures. Aperture corrections have been derived from stellar sources in the mosaicked data by the instrument teams, and these have been applied to correct to total fluxes. The IRAC flux calibration is believed to be correct within 3%, and the 24 μm calibration to 10%. There is an additional scatter resulting from color dependencies in the flat field that add a $\lesssim$10% random error to the fluxes for all IRAC data. The calibration was confirmed for IRAC by comparison with the Two Micron All Sky Survey (2MASS), a robust extrapolation from the 2MASS *K*-band, since the IRAC bands lie on the Rayleigh-Jeans tail of the stellar spectral energy distribution (SED). For 10 stars in our field with 2MASS magnitudes, we extrapolated to a 24 μm flux density using Kurucz-Lejeune atmospheric models for MK class I, III, and V implemented in the *Spitzer* Science Center (SSC) stellar performance estimation tool, assuming G5 spectral type, confirming the calibration to better than 10%. The resulting catalogs were examined by eye and remaining spurious sources (from radiation, scattered light, etc.) were removed by hand. Details of the data processing are given in J. Surace et al. (2004, in preparation) and J. Shupe et al. (2004, in preparation).

The optical g', r', and i' data were taken in 2002 February and the *U* data in 2004 January using the MOSAIC camera on the Mayall 4 m telescope at Kitt Peak National Observatory (B. Siana et al. 2004, in preparation). The data were processed with the Cambridge Astronomical Survey Unit's reduction pipeline following the procedures described by Babbedge et al. (2004). Fluxes were extracted within 2.″06 apertures and corrected for the aperture using profiles measured on bright stars. An analysis comparing the 2.″06 aperture-corrected magnitudes with total "Kron" magnitudes in the r' band indicated that at brighter than $\sim$21.5 mag (Vega), significant numbers of galaxies have fluxes underestimated by the aperture photometry, and therefore our analysis is limited to galaxies fainter than this limit. Colors for the source samples were constructed from the aperture-corrected magnitudes.

The final depths for the *Spitzer* sample, at $\sim$5 times the noise level, are given in Table 1. These depths are consistent with the 90% completeness limits as determined from the deviation of the observed number counts from a power law, and from simulated extractions of artificial sources injected into the data. The median achieved depths for extended objects (galaxies) in the optical bands, at the $\sim$90% completeness levels for source extraction, derived in a similar fashion to the *Spitzer* data, are $U = 24.9$, $g' = 25.7$, $r' = 25.0$, and $i' = 24.0$.

Stars were removed statistically from the *Spitzer* catalog using predicted counts based on a near-infrared (NIR) Galactic stellar distribution model by Jarrett et al. (1994), based on the classic optical model of Bahcall & Soneira (1980). The model was verified using optical stellarity measures for objects associated with IRAC sources, and by matching star counts within a deep 2MASS catalog which reaches $\sim$2 mag fainter than the all-sky 2MASS survey (Beichman et al. 2003). Stars outnumber galaxies at $F_{3.6\,\mu\mathrm{m}} \gtrsim 150$ μJy at this latitude (J. Surace et al. 2004, in preparation) and decrease rapidly in number relative to galaxies below that flux density.

2. RESULTS AND DISCUSSION

The detection statistics in Table 1 indicate that over the full SWIRE survey area of $\sim$49 deg^2, we will detect $\sim$2.4 million galaxies at 3.6 μm and $\sim$120,000 in all four IRAC bands. At 24 μm the detection rate for the full survey will be better than for the VF discussed here because MIPS integration time has been doubled; therefore we estimate nearly 350,000 galaxies detected in this band, and about 70,000 of these in all four IRAC bands as well. At optical wavelengths we detect 27,911, 42,817, 39,308, and 30,230, stars plus galaxies at *U*, g', r', and i', respectively; 17,894 are detected in all four optical bands; 8626 in the combination r', 3.6 μm, 4.5 μm; and 325 are detected in all nine optical+IR bands.

We have compared the IR detection statistics to predictions from the models of Xu et al. (2003), model S3+E2, in Table 1. Model S3 includes dusty objects (spirals, starbursts, and AGNs), and E2 contains passively evolving stellar systems, i.e., spheroids. The Xu et al. model overpredicts SWIRE IR galaxy numbers by a factor of $\sim$2 in the IR bands. The number counts results will be addressed by J. Surace et al. (2004, in preparation) and J. Shupe et al. (2004, in preparation).

Figures 2 and 3 present color-color plots that characterize the sample in g' to 24 μm color-color space. Only sources detected in all four bands shown in each figure are plotted; no limits are shown, for clarity. The figures show SED-redshift tracks of several galaxies with a broad range of intrinsic colors. These SEDs cover the range of colors exhibited by known objects throughout the *U*–24 μm wavelength range and $0 < z < 2$. We do not expect many sources in the region of the figures occupied by rare objects like Arp 220 at low redshift, because our volume coverage at low-redshift space is small. A complete analysis of SWIRE galaxy colors relative to model predictions and SED tracks is beyond the scope of this paper, requiring thorough analysis of selection effects, photometric redshifts and *K*-corrections. Here we note a few basic results.

There is a very broad distribution of colors in these figures. Galaxies with little ongoing star formation will be relatively blue in the mid-IR because of a lack of dust emission, and also quite red in $g'-r'$ because of domination by late-type stars,

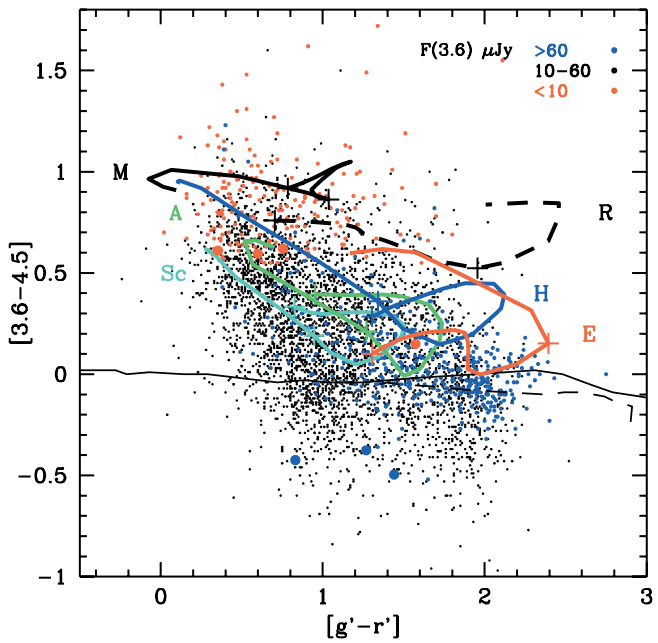

FIG. 2.—Color-color distributions for 4395 sources detected at g', r', 3.6 μm, and 4.5 μm with S/N > 10 and $r' \geq 21.5$. Sources with upper limits are not shown, for clarity. Stellar tracks are shown for main sequence (*light solid black line*) and giants (*light dashed black line*). Galaxy SEDs, $0.1 < z < 2$, with crosses at $z = 0.1$ and 1, are shown for elliptical (*red line*, E); Sc spiral (*cyan line*, Sc); Arp 220 (*green line*, A); the well-known ULIRG and QSO Mrk 231 (*heavy solid black line*, M); an ERO, HR 10 (*blue line*, H); and a red QSO discovered in the FIRST survey (*heavy dashed black line*, R; FIRST J013435.7−093102; optical/NIR spectrum from Gregg et al. [2002]; at longer wavelengths the IR spectrum of PG 1351+236, which has a very similar optical/NIR spectrum, was added by M. Polletta et al. 2004, in preparation). Units are Vega magnitudes, using zero points of 277.5, 179.5, 116.6, 63.1, and 7.3 Jy at 3.6, 4.5, 5.8, 8, and 24 μm, respectively. Large filled dots indicate objects illustrated in Fig. 4 that are detected in each band depicted in this figure: blue symbols are for objects with $[3.6] - [4.5] < -0.3 (F_{3.6\,\mu m}/F_{4.5\,\mu m} > 2.0)$, and red symbols are for objects with $[3.6] - [24] > 7.5$ mag $(F_{3.6\,\mu m}/F_{24\,\mu m} < 0.04)$.

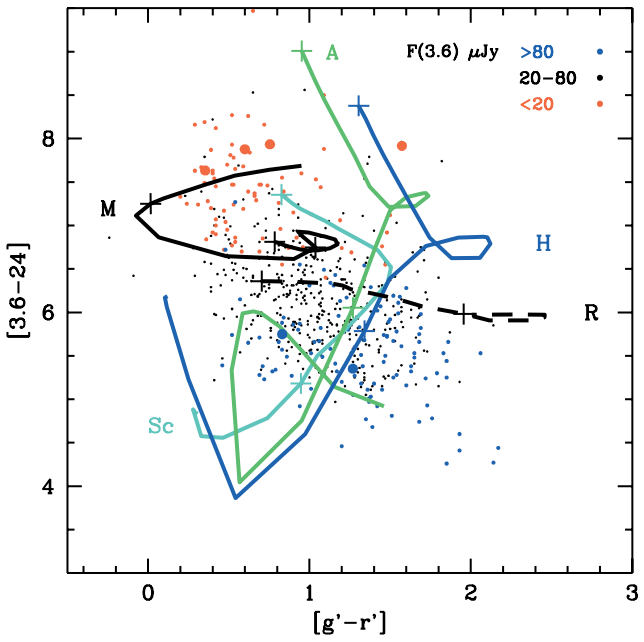

FIG. 3.—Color-color distributions for 588 sources detected at g', r', 3.6 μm, and 24 μm with S/N > 5 and $r' \geq 21.5$. Tracks and symbols are as for Fig. 2, except Mrk 231 has been extended to $z = 3$, with an additional marker plotted at $z = 2$.

and thus will be found toward the lower right of Figure 2, near the elliptical SED track (*red curve*). Indeed, there is a concentration of systems near this region. Moreover, the systems in the sample brightest in 3.6 μm (*blue symbols*) preferentially inhabit this region, indicating that these may be relatively nearby early-type systems. The stellar tracks also cross this region of Figure 2; using the stellar model described above we predict a maximum 0.13 star fraction in the $10 < F_{3.6\,\mu m} < 150$ μJy flux range, and 0.09 for $7.3 < F_{3.6\,\mu m} < 10$ μJy, focused strongly within ± 0.2 mag of the stellar sequences. In Figure 3 the elliptical SED track lies off the figure to the bottom, as a result of a lack of 24 μm emission; objects in this lower right area are likely to be early-type spirals or unusually dusty spheroids.

Dusty systems will be more strongly detected at the longer wavelengths and therefore redder in the *Spitzer* [3.6]−[4.5] and [3.6]−[24] colors. There is a trend in both figures that these systems also tend to be the bluest in $g'-r'$, inhabiting the upper left of both figures. This is expected for systems that have both young complexes of dust-enshrouded star formation dominating the mid-IR and either (1) hot blue young stars visible in lower optical depth regions at optical wavelengths, or (2) a blue type 1 AGN visible in the optical, such as Mrk 231, which tracks into this area at $z > 2$ in Figure 3. It is notable that the most extreme systems (those toward the upper left of the figures), tend to be the fainter galaxies in the sample at 3.6 μm (*red symbols*). This could be interpreted as due to either preferentially more distant systems or lower luminosity systems; however, the complex selection and *K*-correction effects would need to be understood in order to investigate this further.

Some areas of the color-color diagrams are not well covered by the SED tracks. Of particular note are some unusually blue objects in [3.6]−[4.5], and mid-IR red sources at the upper left of Figure 3. Many additional extreme-colored objects with upper limits in one or more color are not shown in these figures. As an illustration of some of the most unusual objects populating the SWIRE sample, we have investigated a number of these sources with red [3.6]−[24] colors and unusually blue [3.6]−[4.5] colors, using the photometric redshift code *Hyper-z* (Bolzonella et al. 2000) to fit SEDs with a wide range of templates, redshifts, and A_V. We used our own library (M. Polletta et al. 2004, in preparation), the GRASIL library (Silva et al. 1998), and the Rowan-Robinson (2003) library. The Polletta et al. library contains around forty 1000 Å–20 cm templates for ellipticals, spirals, irregulars, starbursts, ultraluminous infrared galaxies (ULIRGs), and AGNs, derived from observed SEDs, including mid-IR *Infrared Space Observatory* (*ISO*) spectra and models following Berta et al. (2004). A more complete characterization and photometric redshift analysis of a larger SWIRE galaxy sample will be forthcoming (M. Rowan-Robinson et al. 2004, in preparation).

Investigating first the blue sources, we selected 603 sources with $[3.6] - [4.5] < -0.3$, significantly bluer than normal galaxies and stars, with S/N ≥ 10 in both bands. Fluxes were remeasured by hand for 193 of these objects with detections in a sufficient number of bands for SED analysis. We used the IPAC *Skyview* software to set background levels interactively, thus avoiding confusion with nearby sources and background contamination. In all, 67 sources were found to have valid colors. In about 8% of the remaining cases, the automated

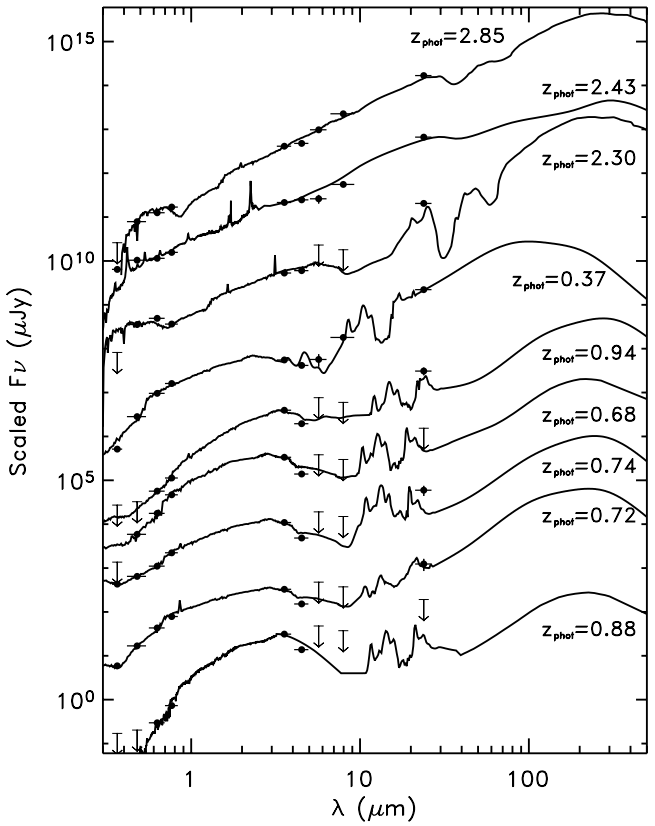

FIG. 4.—SEDs for five sources with $[3.6] - [4.5] < -0.3$ (lower five SEDs) and four sources redder than $[3.6] - [24] = 7.5$ mag. In most cases the uncertainties are smaller than the symbol sizes.

source extractor measured a different region of a close or confused pair of sources, or of an extended source, in the two bands. Here 32% of the sources marginally miss the color cut on careful color reevalution, 8% are cosmic rays or bad pixels, 36% have anomalous 3.6 μm fluxes caused by local background or other effects due to bright stars, and 16% have anomalous fluxes at either 3.6 or 4.5 μm with no obvious explanation. The last three categories represent a $76/12784 = 0.6\%$ anomaly rate among the entire $S/N > 10$ 3.6 μm catalog, and a 40% anomaly rate among the $[3.6] - [4.5] < -0.3$ sample. Since anomalies are preferentially expected among odd-colored sources, the high anomaly rate among the unusually blue sources is not unanticipated.

The 67 valid $[3.6] - [4.5] < -0.3$ objects exhibit a wide range of optical to mid-IR colors. Seven are relatively blue and pointlike throughout the optical and mid-IR, and are probably stars. None of the galaxy libraries contains any templates as blue as the remaining $[3.6] - [4.5] < -0.3$ sources at any redshift. Two objects in the literature have colors possibly as blue at 3–5 μm: the peculiar QSO [HB89] 0049−29 at $z = 0.308$ (Andreani et al. 2003), and the Seyfert 2 ULIRG IRAS 00198−7826 at $z = 0.073$ (Farrah et al. 2003). [HB89] 0049−29 peaks strongly in the NIR; however, it is very red from there into the optical, unlike any of our sources. IRAS 00198−7826 is not observed at these wavelengths, but is predicted to be as blue as our sources (Farrah et al. 2003), which is explained by it being a $\gtrsim$60 Myr starburst in which much of the gas and dust has been blown away by supernovae. This model for IRAS 00198−7826 can produce colors similar to those of our blue objects in the [3.6]−[4.5] color, but it is too blue into the optical to match any of our sources at any redshift.

Another possible explanation for the blue [3.6]−[4.5] colors is a strong 3.3 μm polycyclic aromatic hydrocarbon (PAH) feature in the 3.5 μm band at low redshift ($<$0.1), but it would have to be considerably higher equivalent width than any such feature found in any of our templates. Also possible is a strong 2.35 μm CO bandhead absorption moving into the 4.5 μm filter at redshift $\sim$0.7, requiring a young stellar population of red supergiants that is not diluted strongly by an older stellar population with a weaker absorption (Rhoads 1997). This might perhaps indicate a dominant $\sim 10^7$ yr old starburst in a fairly low mass galaxy. Alternatively, such a high equivalent width may indicate low metallicity.

In Figure 4 and Table 2 we present representative best fits for five blue sources (lower five SEDs; first five table entries). The 24 μm data points were downweighted in these fits so that they would not throw off the fit in the 3–5 μm region, with which we are primarily concerned here; mid-IR SEDs can have a wide range of shapes depending on details of geometry and astrophysics, which cannot be encapsulated in small libraries. The fitted redshifts range from 0.68 to 0.94, and the corresponding infrared luminosities range from $\log L_{3-1000\,\mu m} = 10.3$ to 11.3 $L_\odot$;[15] these are star-forming galaxies and starbursts at moderate redshifts with moderate luminosities. The blue [3.6]−[4.5] region of the SED is only approximately fit, as anticipated, with deviations 0.8 to 2.2 σ high for the 3.6 μm points, and 4.3 to 7.9 σ low for the 4.5 μm data points (combined deviations of the [3.6]−[4.5] color from the template are given in the last column of Table 2). We present

[15] $H_0 = 71$ km s^{-1} Mpc^{-1}, $\Omega_m = 0.27$, $\Omega_\Lambda = 0.73$.

TABLE 2
SELECTED SOURCES WITH UNUSUALLY BLUE [3.6]−[4.5] OR RED [3.6]−[24] COLORS

Name	R.A. (J2000)	Decl. (J2000)	z_{phot}	$L_{3-1000\,\mu m}$ ($L_\odot$)	A_V (mag)	Template	Deviation σ, Blue Sources
SWIRE_J104513.3+585933	10 45 13.39	58 59 33.5	0.88	10.3	0.8	Sa	7.2
SWIRE_J104552.8+590600	10 45 52.86	59 06 00.8	0.72	11.3	1.0	Sd pec	7.2
SWIRE_J104657.3+590902	10 46 57.38	59 09 02.5	0.74	10.9	0.2	Sdm	4.6
SWIRE_J104743.7+591034	10 47 43.75	59 10 34.6	0.68	10.8	0.5	Sbc H II	8.4
SWIRE_J104436.8+591349	10 44 36.84	59 13 49.2	0.94	11.2	1.3	Sc starburst	6.2
SWIRE_J104616.0+591424	10 46 16.08	59 14 24.9	0.37	11.1	0.8	Im pec H II	...
SWIRE_J104511.8+590121	10 45 11.88	59 01 21.6	2.30	13.4	0.2	H II	...
SWIRE_J104613.4+585941	10 46 13.44	58 59 41.3	2.43	13.2	1.1	QSO	...
SWIRE_J104700.2+590107	10 47 00.20	59 01 07.6	2.85	13.7	0.3	Sy1	...

these fits as illustrative and not unique; fits at substantially different redshifts are possible with different combinations of templates and A_V values. If this phenomenon is confirmed as a real and substantial population with unusually blue 3−5 μm SEDs, ideal fits will require modified template modeling outside the current libraries. We note that the fitted redshifts for all of these objects are consistent with the hypothesis of a dominant population of red supergiants with strong CO absorption at 2.35 μm redshifted into the 4.5 μm band. It will be most interesting to discover whether *Spitzer* finds similarly blue colors in any regions within nearby galaxies, where the stellar populations and interstellar medium can be investigated in some detail.

We have also selected all sources redder than $[3.6] - [24] = 7.5$ mag for investigation (see Fig. 3), requiring a detection at $S/N > 5$ at 24 μm. Of 63 sources with $[3.6] - [24] > 7.5$ mag, 42 were found to have valid colors this red on rederivation of their fluxes by hand. The remainder are about evenly divided between sources for which more than one 3.6 μm source likely contributes to the larger beam 24 μm emission (a commonly expected situation due to the large difference in beam profiles), and spuriously low 3.6 μm flux densities caused by latents or electronic offsets due to nearby bright stars. This latter category of anomalies at 3.6 μm represents a $10/16075 = 0.06\%$ anomaly rate among the whole catalog, and 17% among the selected red sources. As for the unusually blue [3.6]−[4.5] sources, a high anomaly rate among color outliers is not unanticipated.

The best-fit redshifts for four representative red sources (Fig. 4, upper four SEDs; Table 2, last 4 entries) range from 0.37 to 2.85, with a luminosity range of $\log L_{3-1000\,\mu\mathrm{m}} = 11.1$ to 13.7 $L_\odot$. It is very difficult to obtain unique fits for some objects of this type owing to the flatness of the SEDs and the limited number of data points, and these fits should be regarded as illustrative only, pending a thorough analysis of the possible range of templates, redshifts, and luminosities that can fit each of these sources. These objects appear to be starbursts, ULIRGs, and AGNs with a wider redshift and luminosity range than the blue sources in Figure 4, including some $z > 2$ objects with luminosities in the hyperluminous object (HyLIRG) range. SWIRE is expected to be particularly sensitive to high-redshift IR-luminous AGNs, which are expected to be bright in the very sensitive 24 μm band because of warm circumnuclear dust. The high-redshift volume density of HyLIRGs will be important for models for the early formation of massive systems in the universe. *Spitzer* IRS spectroscopy may prove essential for determining redshifts and excitations for the reddest, optically faintest systems.

Support for this work, part of the *Spitzer Space Telescope* Legacy Science Program, was provided by NASA through an award issued by the Jet Propulsion Laboratory, California Institute of Technology under NASA contract 1407.

REFERENCES

Andreani, P., Cristiani, S., Grazian, A., La Franca, F., & Goldschmidt, P. 2003, AJ, 125, 444
Babbedge, T. S., et al. 2004, MNRAS, in press (astro-ph/0406296)
Bahcall, J. N., & Soneira, R. M. 1980, ApJS, 44, 73
Beichman, C., Cutri, R., Jarrett, T., Steining, R., & Skrutski, M. 2003, AJ, 125, 2521
Berta, S., Fritz, J., Franceschini, A., Bressan, A., & Lonsdale, C. 2004, A&A, in press
Bolzonella, M., Miralles, J.-M., & Pelló, R. 2000, A&A, 363, 476
Farrah, D., Fox, M., Efstathiou, A., Afonso, J., Clements, D., & Rowan-Robinson, M. 2003, MNRAS, 343, 585
Gregg, M. D., Lacy, M., White, R. L., Glikman, E., Helfand, D., Becker, R. H., & Brotherton, M. S. 2002, ApJ, 564, 133
Jarrett, T. H., Dickman, R. L., & Herbst, W. 1994, ApJ, 424, 852
Lonsdale, C., et al. 2003, PASP, 115, 897
Oliver, S., et al. 2004, ApJS, 154, 30
Rhoads, J. 1997, in Extragalactic Astronomy in the Infrared, ed. G. Mamon, T. X. Thuan, & J. Tran Than Van (Paris: Edition Frontières), 45
Rowan-Robinson, M. 2003, MNRAS, 345, 819
Silva, L., Granato, G. L., Bressan, A., & Danese, L. 1998, ApJ, 509, 103
Xu, C. K., Lonsdale, C. J., Shupe, D. L., Franceschini, A., Martin, C., & Schiminovich, D. 2003, ApJ, 587, 90

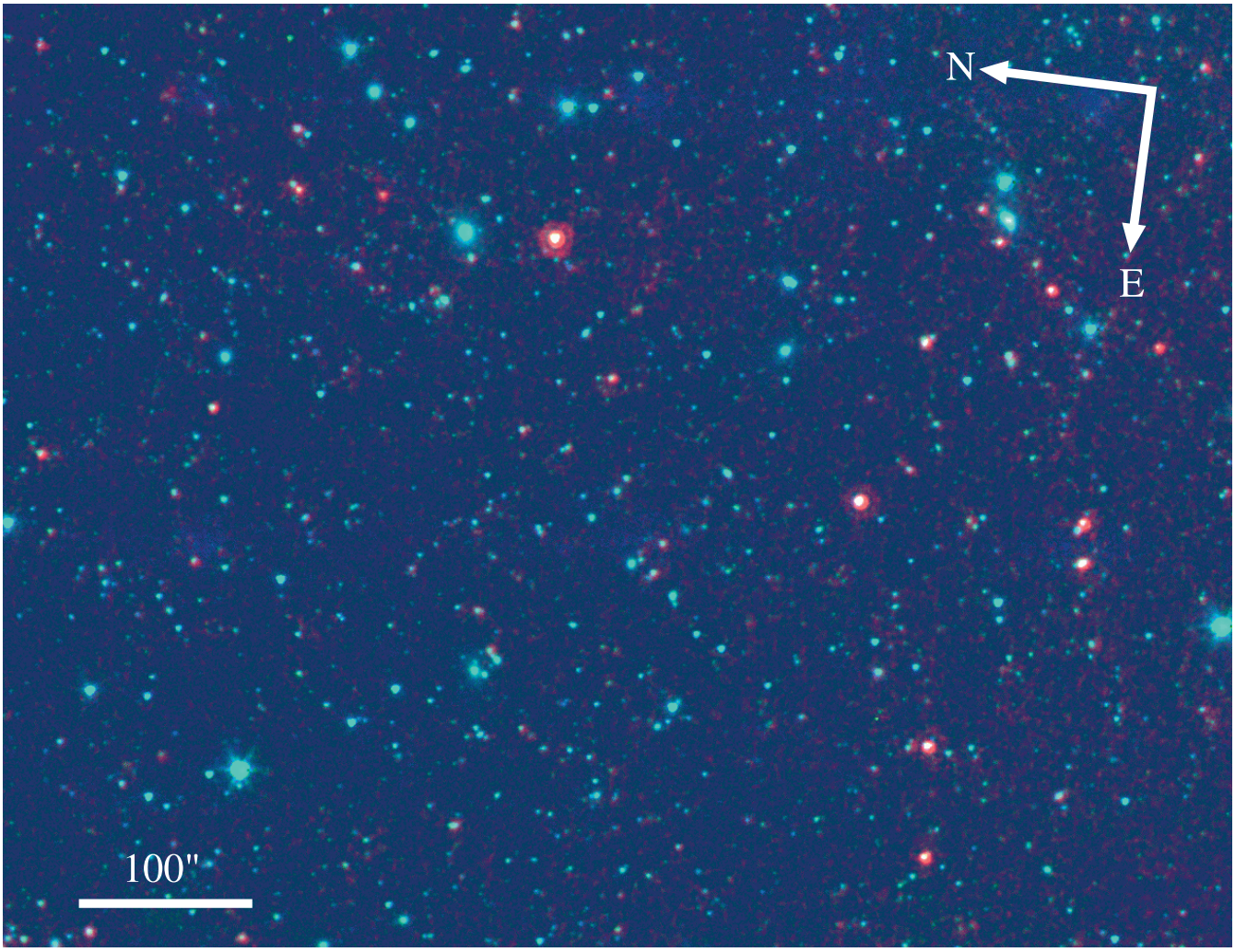

FIG. 1.—Three-color image of ~0.03 deg^2 of the SWIRE Lockman validation field, centered at $10^h47^m32\overset{s}{.}67$, $59°07'16\overset{''}{.}3$, showing 3.6 μm (*blue*), 4.5 μm (*green*), and 24 μm (*red*).

PLATE 1